Optical properties of alkali-antimonite glasses and purified processes for fiber drawing

Mohamed Baazouzi, Mohamed-Toufik Soltani, Majda Hamzaoui, Marcel Poulain, Johann Troles

Optical properties of alkali-antimonite glasses and purified processes for fiber drawing

M.Baazouzi[1,2], M.T.Soltani[2], M.Hamzaoui[1,2], M. Poulain[1], J. Troles[1*]

[1] *Equipe Verres et Céramiques, UMR-CNRS 6226, Sciences Chimiques de Rennes, Université de Rennes I, 35042 Rennes Cedex, France*

[2] *Laboratoire de physique photonique et nanomatériaux multifonctionnels, Université de Biskra BP 145 RP, 07000 Biskra, Algeria*

* *Corresponding author, Johann.troles@univ-rennes1.fr*

ABSTRACT

We study Antimonite glasses in the ternary systems Sb_2O_3-PbO-M_2O (M=Li, Na, K). We have measured the density and refractive index according to the glass composition in this system. We have also measured the optical transmission in the UV-Vis and infrared range and the optical band gap. The influence of glass synthesis on extrinsic absorption has been studied. For the first time in this system, we have observed that stable glassy composition was drawn into a fiber, and the optical losses were determined in the 1-5 µm infrared regions.

1. INTRODUCTION

[Texte]

Heavy metal oxide glasses are known for their large transparency window, their high refractive index and their strong non-linear optical properties. Indeed, heavy metal oxide glasses are transparent from the visible region up to 5-6 µm in the mid infrared, depending on the composition [1-4]. In addition, glasses containing highly polarizable element presents also high linear and nonlinear refractive index [5]. As example, lead silica glasses can have a nonlinear refractive index n_2 ten times higher than the n_2 of fused silica [6]. In non-silica glasses, for example tellurite glasses based on TeO_2, the value of the n_2 can be 20-30 times higher than in pure silica [7, 8]. Antimony oxide Sb_2O_3 is a glass progenitor that leads to numerous vitreous systems. Such original glasses are similar to tellurite glasses and present also a real interest for nonlinear applications and for rare earth doped glasses [9-11]. It can be noticed that combining high nonlinear properties and IR transmission is very attractive for the realization of new super-continuum IR sources [12-14].

While the formation of vitreous Sb_2O_3 is still a matter of discussion, numerous binary and multicomponent glasses based on this oxide have been reported [4, 15-18]. Incorporation of silica or phosphate enhances vitrification but it also increases phonon energy, which leads to reduced infrared transmission and modifies the spectroscopic influence of the matrix on doping ions [19, 20]. Previous study has shown large vitreous domain in the ternary system Sb2O3-PbO-M2O, where M is alkali metal such as Li, Na, and K [17]. In [5], highly stable antimonite glasses doped Er were prepared and found to be promising visible and infrared amplifiers materials

In this paper, firstly, we investigate the optical properties: refractive index, optical band gap, impurities absorption bands. Secondly, we achieve different processes to obtain high quality glasses. And finally we realize the fibering of a purified glass and we measure the losses of the fiber.

2. EXPERIMENTAL

2-1 Glass synthesis

Three glassy systems have been studied: Sb_2O_3 - PbO - M_20 (M = Li, Na and K). In order, to investigate the role of the alkali and the PbO content on the optical properties, five compositions with the same ratio (Sb_2O_3/M_2O) have been studied in each ternary system (figure 1). The glasses are labeled SLPx, SNPx, and SKPx with S = Sb_2O_3, L=Li_2O, N=Na_2O, K=K_2O, and P = PbO, where x indicates the molar concentration in mol % of PbO (x= 0 to 20). In addition, purification processes have been investigated on the $(Sb_3O_2)_{80}(PbO)_{10}(K_2O)_{10}$ glass. This composition has been chosen for its high thermal stability suitable with drawing operation.

The starting materials (Sb_2O_3, K_2CO_3, Na_2CO_3, Li_2CO_3 and PbO) are supplied by (Alpha Aesar), with a 99.999% purity. For the first part of this study, the antimonite glasses were synthesized in silica tube in air. The starting raw materials (5 g) are firstly mixed and placed in a 16 mm diameter silica tube. The mixture is then flame heated during 5 to 10 min until a homogeneous liquid is obtained. Then, the melt is casted onto a brass plate at 250°C. Synthesis temperatures vary from 800°C to 1100°C according to the alkali content. During the melting, alkali oxides are formed through the chemical reaction between alkali carbonate and antimony oxide, resulting in CO_2 release.

During the synthesis in silica crucible in ambient air, the glass melt reacts with the crucible and reacts also with the atmosphere moisture. As a result, strong absorption bands due to O-H and Si-O vibrations are observed in the infrared spectrum. In order to avoid those parasitic bands, different synthesis methods have been investigated. So, before the elaboration of an optical fiber, purification processes have been achieved on the $(Sb_3O_2)_{80}(PbO)_{10}(K_2O)_{10}$ glass composition.

[Texte]

Firstly, a glass has been prepared in alumina crucible in air and second one in the same crucible in neutral atmosphere (in a glove box; under Ar). And in another set of preparations, syntheses have been achieved under vacuum (10^{-3} mbar). In a first synthesis, the raw materials are placed directly in the silica ampoule. In a second step, in order to avoid chemical reactions between silica crucible and the glass melt, the mixture is placed into an alumina crucible placed itself in a silica ampoule. In both syntheses, the batch is heated under vacuum at 200 ° C for 1 h in an electric oven to ensure efficient water desorption. Then, the temperature is increased up to 500 - 550 ° C during 2 h, to obtain a total alkali decarbonation. After the decarbonation, the reactional ampoule is obtained by sealing the silica tube. Then, the sealed ampoule is slowly heated in an electric furnace up to the temperature of homogenization (600 °C). The batch is kept at this temperature for 4h. Finally, the melt is quenched in water at room temperature. The glass is then annealed around the glass transition (T_g -10 ° C) to reduce the mechanical stresses induced by the quenching. On can note, even during the vacuum processes, no significant changes have been observed on nominal composition of the purified glasses.

2-2 Physical measurements

Thermal properties are measured by differential scanning calorimetry (DSC Q20 equipment) with a heating rate of 10° C/min. The estimated error is 2 °C for glass transition T_g and onset of crystallization T_x. Characteristic temperatures are measured up to 550 °C. The density of glasses is measured in a helium picnometer (Micromeritics, AccuPyc 330). The compositional dependence of the different physical measurements is reported in table 1. Optical properties have been also investigated. The external absorption bands such as Si-O and OH^- related to the glass synthesis are measured in the infrared range and were recorded in a BRUKER (Tensor 37) Michelson Spectrophotometer in the 400–4000 cm^{-1} range. The refractive index

of all the glasses is measured by Metricon Model 2010 / M. The wavelength associated to the optical band gap of the glasses has been computed by absorption measurement by using a Perkin Elmer spectrometer (Lamba 1050). In this paper, the wavelength corresponding to the band gap is given when the absorption of the glass reaches 10 cm^{-1}. The optical properties of the different samples studied (refractive indices and band gap wavelength) are listed in table 2

3. RESULTS AND DISCUSSION

The thermal properties measured by DSC are presented in table 1. The glass transition (T_g) varies from 265 to 285 °C. One can note a small variation of the glass transition with the composition. All samples have shown a crystallization peak (T_x) which occurs when the temperature reaches 100-200 °C above the T_g, depending on the composition. The thermal stability factor of glasses is currently estimated by calculating $\Delta T=T_x-T_g$. The obtained ΔT in the [100-200°C] range indicates a good stability of these glasses [21]. Glasses containing the potassium oxide exhibit higher ΔT especially for high amount of lead oxide. For this reason, the $(Sb_3O_2)_{80}(PbO)_{10}(K_2O)_{10}$ glass has been chosen for fiber drawing.

The densities of the studied glasses are reported in table 1 and its variation versus composition is shown in Fig. 2. The density values vary from 4.5 $g.cm^{-3}$ to 5.4 $g.cm^{-3}$. In all glassy systems, density increases with lead oxide addition. Note that the density also increases when the atomic weight of the alkali cation decreases. This results from the decrease of the molar volume in relation to the reduction of alkali size.

The measured refractive indices in the Sb_2O_3-PbO-M_2O system vary between 1.9 to 2.1 depending on wavelength and on composition. The higher values are observed in the Sb_2O_3-PbO-Li_2O system. As an example, the refractive index at 632 nm of the SLP 20 with 20 % of lead oxide reaches 2.1. In each ternary system, the increase of the density implies the increase

of the refractive index. It is not surprising that the density, and with it the refractive index, both increase with the concentration of lead oxide (Fig. 3).

The optical transmission spectra in the infrared region (2.5-8 µm) has been studied for the $(Sb_3O_2)_{80}(PbO)_{10}(K_2O)_{10}$ in order to improve the optical quality of the glasses (Fig4). When the sample is synthesized in air and in a silica crucible, the infrared spectrum exhibits two strong absorption bands at 3.1 µm and 5.5 µm (Fig 4, table 3). These absorption bands are attributed to O-H and Si-O chemical bonds respectively. The infrared signature of the O-H groups at 3.1 µm indicates a water contamination of the sample. This water contamination has two different origins: water adsorbed by the raw materials and contamination by air moisture during synthesis. In order to avoid this water pollution, a glass has been prepared in a SiO_2 crucible under vacuum (decarbonation and melting). This procedure permits to reduce the O-H absorption band from 4.65 to only 0.21 cm^{-1} (table 3). However, the IR transmission is still limited by the contamination of the sample with Si-O group from the crucible. One may assume that silicon oxide (SiO_2) arising from crucible contamination can help the glass formation. Nevertheless, several synthesis have been successfully carried out in alumina crucible (in air, in Argon glove box and under vacuum). Consequently the Si-O absorption band has been completely eliminated, and the cut-off wavelength in the infrared region has been found to achieve 7.5 µm as seen in figure 4. The presence of Si has been also confirmed by energy dispersive X-ray spectroscopy in sample prepared in SiO_2 crucibles. Finally, a glass has been prepared (decarbonation and melting) under vacuum in an alumina crucible. In this case, the glass shows only a small O-H absorption band with an absorption coefficient around 0.1 cm^{-1}. This procedure has been chosen for the realization of the glass rod used for the fiber drawing. Indeed, the $(Sb_3O_2)_{80}(PbO)_{10}(K_2O)_{10}$ composition has been drawn into a fiber with a diameter equal to 300 µm. The transmission loss spectrum has been measured by using the cut back method with 1 meter long fiber (Figure 5). The attenuation reaches 4 dB/m in the 1-2.5

µm region, while optical losses increase strongly beyond 2.5 µm because of residual O-H groups. The absorption coefficient at 3.1 µm can be estimated around 60 – 80 dB/m, that is from 0.14 cm^{-1} to 0.18 cm^{-1}. This value is closed to the value observed in the bulk glass (0.10 cm^{-1}). For optical applications, the optical quality has to be improved. However, this makes the first report of an optical fiber composed of Sb_2O_3, PbO and K_2O.

4. CONCLUSION

Sb_2O_3-based glasses in the ternary systems Sb_2O_3-PbO-M_2O (where M=Li, Na or K) have been synthesized and characterized. The glasses are stable at room atmosphere and their devitrification tendency upon cooling is limited. Their density is about 5 g/cm^3 and the refractive index varies from 1.9 to more than 2.1 at 632.8µm depending on alkali or lead oxides contents. In this paper, we investigate the optical properties of these glasses, namely the optical band gap wavelength and the optical transmission in the infrared window. Various impurities and defects limit the optical quality of the current samples; this quality has been significantly improved by optimizing glass processing. An optimized glass rod has been drawn into an optical fiber with optical attenuation close to 4 dB/m in the 1-2.5 µm region. Optical losses increase beyond 2.5 µm because of residual O-H groups. This achievement makes the first realization of a fiber in this glassy system, which appears promising for future developments. These glasses could have potential applications as low phonon energy glasses for infrared transmission or infrared active devices.

REFERENCES

[1] W. H. Dumbaugh and J. C. Lapp, J. Am. Ceram. Soc 75 (1992) 2315.
[2] C. J. Hill and A. Jha, J. Non-Cryst Solids 353 (2007) 1372.
[3] K. Nassau, D. L. Chadwick and A. E. Miller, J. Non-Cryst Solids 93 (1987) 115.
[4] G. Poirier and M. Poulain, J. Non-Cryst Solids 284 (2001) 117.
[5] E. M. Vogel, M. J. Weber and D. M. Krol, Phys. Chem. Glasses 32 (1991) 231.
[6] J. H. V. Price, T. M. Monro, H. Ebendorff-Heidepriem, F. Poletti, P. Horak, V. Finazzi, J. Y. Y. Leong, P. Petropoulos, J. C. Flanagan, G. Brambilla, M. Feng and D. J. Richardson, IEEE J. Sel. Top. Quant 13 (2007) 738.
[7] E. Fargin, A. Berthereau, T. Cardinal, G. LeFlem, L. Ducasse, L. Canioni, P. Segonds, L. Sarger and A. Ducasse, J. Non-Cryst Solids 203 (1996) 96.
[8] I. Savelii, J. C. Jules, G. Gadret, B. Kibler, J. Fatome, M. El-Amraoui, N. Manikandan, X. Zheng, F. Desevedavy, J. M. Dudley, J. Troles, L. Brilland, G. Renversez and F. Smektala, Opt. Mater 33 (2011) 1661.
[9] K. Terashima, T. Hashimoto, T. Uchino, S. H. Kim and T. Yoko, J. Ceram. Soc. Japan 104 (1996) 1008.
[10] L. A. Gomez, C. B. de Araujo, D. N. Messias, L. Misoguti, S. C. Zilio, M. Nalin and Y. Messaddeq, J. Appl. Phys. 100 (2006).
[11] J. S. Wang, E. M. Vogel and E. Snitzer, Opt. Mater. 3 (1994) 187.
[12] P. Domachuk, N. A. Wolchover, M. Cronin-Golomb, A. Wang, A. K. George, C. M. B. Cordeiro, J. C. Knight and F. G. Omenetto, Opt. Express 16 (2008) 7161.
[13] M. El-Amraoui, G. Gadret, J. C. Jules, J. Fatome, C. Fortier, F. Désévédavy, I. Skripatchev, Y. Messaddeq, J. Troles, L. Brilland, W. Gao, T. Suzuki, Y. Ohishi and F. Smektala, Opt. Express 18 (2010) 26655.
[14] R. Gattas, B. Shaw, V. Q. Nguyen, P. C. Pureza, I. D. Aggarwal and J. S. Sanghera, Opt. Fiber Technol 18 (2012) 345.
[15] B. V. Raghavaiah and N. Veeraiah, J. Phys. Chem. Solids 65 (2004) 1153.
[16] M. Nouadji, A. Attaf, R. El Abdi and M. Poulain, J. Alloy. Compd 511 (2012) 209.
[17] M. T. Soltani, A. Boutarfaia, R. Makhloufi and M. Poulain, J. Phys. Chem. Solids 64 (2003) 2307.
[18] B. Dubois, H. Aomi, J. J. Videau, J. Portier and P. Hagenmuller, Mater. Res. Bull 19 (1984) 1317.
[19] T. Som and B. Karmakar, Spectrochim. Acta A 79 (2011) 1766.
[20] M. Czaja, S. Bodyl,, J. Gabrys-Pisarska and Z. Mazurak, Opt. Mater. 31 (2009) 1898.
[21] A. Dietzel, Glasstech. Ber. 22 (1968) 41.

Table 1: Characteristic temperatures and density of the Sb_2O_3 based glasses

Sample	Glass Compositions (mol %)					Temperatures (°C)			Density ($g.cm^{-3}$)
	Sb_2O_3	Li_2O	Na_2O	K_2O	PbO	$T_g \pm 2$	$T_x \pm 2$	(T_x-T_g)	ρ ($\pm$ 0.01)
SKP0	77,78			22,22	0	276	465	189	4,573
SKP5	73,89			21,11	05	272	470	198	4,676
SKP10	70			20	10	270	463	193	4,743
SKP15	66,1			18,9	15	267	467	200	4,897
SKP20	62,2			17,8	20	268	496	228	5,009
SLP0	77,78	22,22			0	277	395	118	4,908
SLP5	73,89	21,11			05	277	407	130	5,040
SLP10	70	20			10	274	416	142	5,140
SLP15	66,1	18,9			15	280	414	134	5,270
SLP20	62,2	17,8			20	271	413	142	5,365
SNP0	77,78		22,22		0	282	446	164	4,761
SNP5	73,89		21,11		05	285	457	172	4,835
SNP10	70		20		10	282	471	189	4,981
SNP15	66,1		18,9		15	282	491	209	5,041
SNP20	62,2		17,8		20	279	384	105	5,143

Table 2: Optical properties: optical band gap and refractive indices

Sample	Refractive Index (±5.10^{-4}) @					Band-Gap* (eV)	Band-Gap wavelength* (nm)
	632,8 nm	825 nm	1061 nm	1311 nm	1551nm		
SKP0	1,9850	1,9550	1,9389	1,9303	1,9256	3.1472	394
SKP5	1,9914	1,9622	1,9459	1,9373	1,9337	3.1234	397
SKP10	1,9907	1,9663	1,9498	1,9403	1,9350	3.0999	400
SKP15	2,0110	1,9801	1,9627	1,9536	1,9486	3.0769	403
SKP20	2,0160	1,9843	1,9671	1,9582	1,9534	3.0617	405
SLP0	2,0602	2,0282	2,0111	2,0023	1,9976	3.1794	390
SLP5	2,0719	2,0426	2,0243	2,0141	2,0084	3.1392	395
SLP10	2,0646	2,0335	2,0156	2,0060	2,0008	3.1313	396
SLP15	2,1060	2,0476	2,0260	2,0179	2,0145	3.0922	401
SLP20	2,1153	2,0583	2,0366	2,0281	2,0244	3.0466	407
SNP0	2,0184	1,9881	1,9703	1,9606	1,9553	3.1234	397
SNP5	2,0163	1,9862	1,9691	1,9601	1,9552	3.1234	397
SNP10	2,0276	1,9951	1,9785	1,9702	1,9659	3.1077	399
SNP15	2,0299	1,9988	1,9817	1,9727	1,9679	3.0999	400
SNP20	2,0357	2,0030	1,9859	1,9772	1,9727	3.0769	403

* The band gap and the band gap wavelength are given when the absorption coefficient reaches 10 cm^{-1}

Table 3: Absorption coefficient for different synthesis processes in the $(Sb_2O_3)_{80}(K_2O)_{10}(PbO)_{10}$ glass

Synthesis	α_{O-H} (cm^{-1})	α_{Si-O} (cm^{-1})
Silica crucible in air	4,65	2,85
Silica crucible under vacuum	0,24	6,64
Alumina crucible in air	3,31	≈ 0
Alumina crucible in Ar glove box	2,12	≈ 0
Alumina crucible under vacuum	0,1	≈ 0

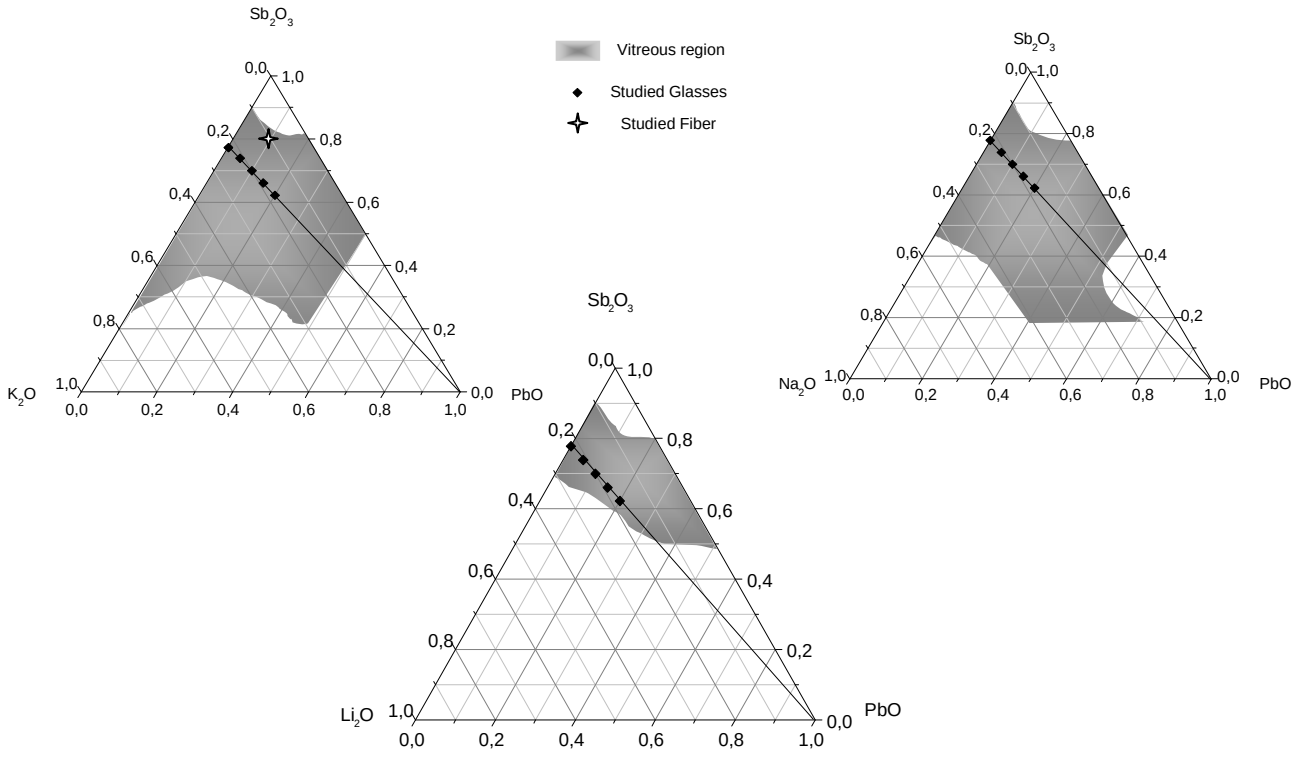

Figure 1: Sb_2O_3-PbO-M_2O (M=Li, Na or K) glassy systems

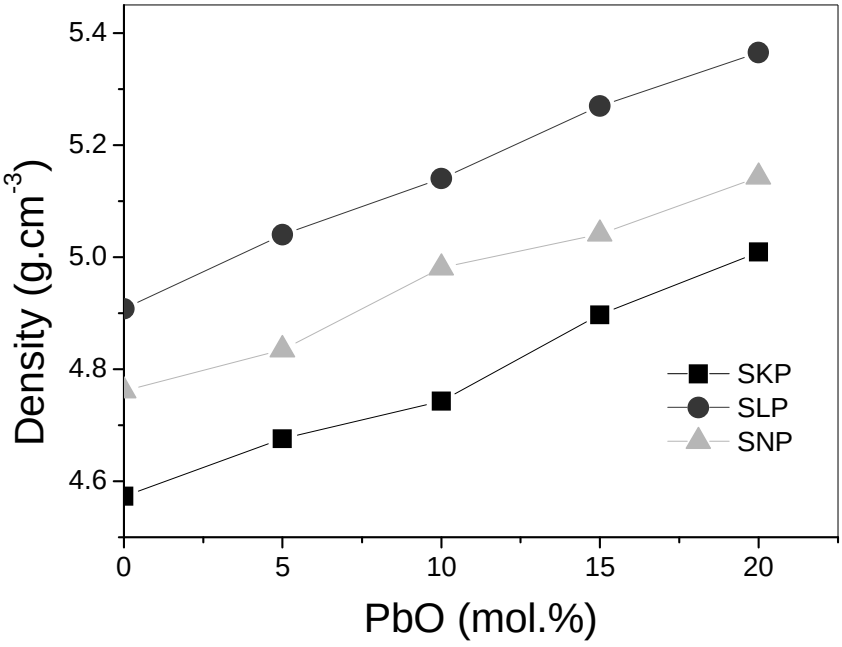

Figure 2: Variation of density with PbO concentration.

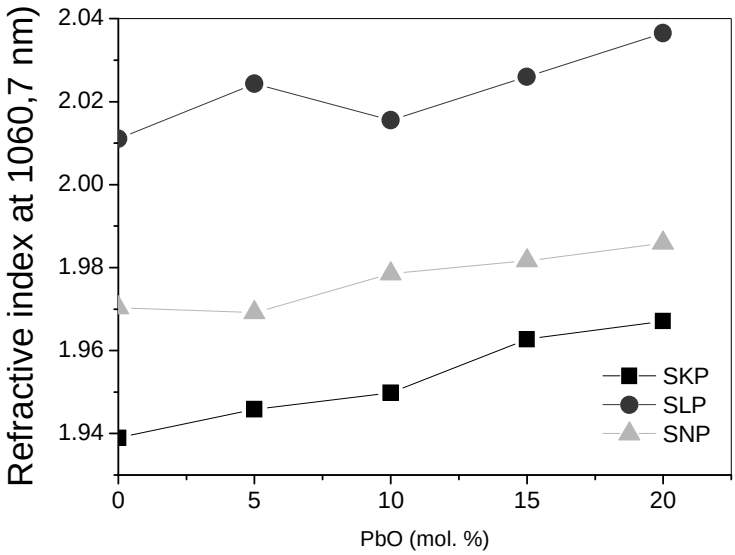

Figure 3: Variation of Refractive Index with PbO Molar Concentration.

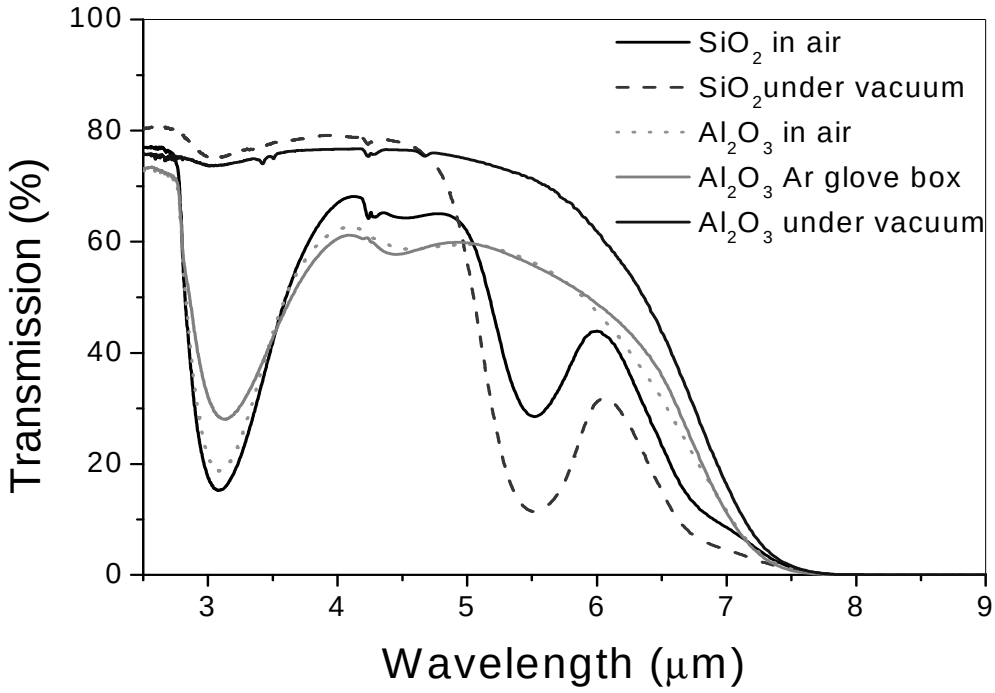

Figure 4: Infrared spectra for different synthesis method (sample thickness ≈ 1 mm)

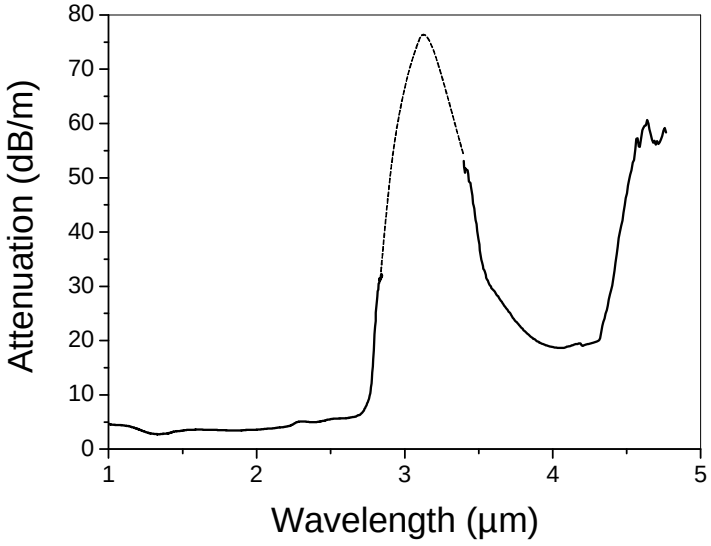

Figure 5: Attenuation curve of a Sb_2O_3 based fiber, the dash curve concerns extrapolated points.